CAP1 binds and activates adenylyl cyclase in mammalian cells

Xuefeng Zhang[a,1], Alejandro Pizzoni[a,1], Kyoungja Hong[a,2], Nyla Naim[a,3], Chao Qi[b], Volodymyr Korkhov[b], and Daniel L. Altschuler[a,4]

[a]Department of Pharmacology and Chemical Biology, University of Pittsburgh School of Medicine, Pittsburgh, PA 15261; and [b]Institute of Molecular Biology and Biophysics, Paul Scherrer Institute, 5232 Villigen PSI, Switzerland

Edited by Robert J. Lefkowitz, Howard Hughes Medical Institute, Durham, NC, and approved May 5, 2021 (received for review November 29, 2020)

CAP1 (Cyclase-Associated Protein 1) is highly conserved in evolution. Originally identified in yeast as a bifunctional protein involved in Ras-adenylyl cyclase and F-actin dynamics regulation, the adenylyl cyclase component seems to be lost in mammalian cells. Prompted by our recent identification of the Ras-like small GTPase Rap1 as a GTP-independent but geranylgeranyl-specific partner for CAP1, we hypothesized that CAP1-Rap1, similar to CAP-Ras-cyclase in yeast, might play a critical role in cAMP dynamics in mammalian cells. In this study, we report that CAP1 binds and activates mammalian adenylyl cyclase in vitro, modulates cAMP in live cells in a Rap1-dependent manner, and affects cAMP-dependent proliferation. Utilizing deletion and mutagenesis approaches, we mapped the interaction of CAP1-cyclase with CAP's N-terminal domain involving critical leucine residues in the conserved RLE motifs and adenylyl cyclase's conserved catalytic loops (e.g., C1a and/or C2a). When combined with a FRET-based cAMP sensor, CAP1 overexpression–knockdown strategies, and the use of constitutively active and negative regulators of Rap1, our studies highlight a critical role for CAP1-Rap1 in adenylyl cyclase regulation in live cells. Similarly, we show that CAP1 modulation significantly affected cAMP-mediated proliferation in an RLE motif–dependent manner. The combined study indicates that CAP1-cyclase-Rap1 represents a regulatory unit in cAMP dynamics and biology. Since Rap1 is an established downstream effector of cAMP, we advance the hypothesis that CAP1-cyclase-Rap1 represents a positive feedback loop that might be involved in cAMP microdomain establishment and localized signaling.

CAP1 | Rap1 | Ras | adenylyl cyclase | cAMP

CAP/srv2 was originally identified in yeast biochemically as an adenylyl cyclase–associated protein (1) and genetically as a suppressor of the hyperactive Ras2-V19 allele (2). CAP/srv2-deficient yeast cells are unresponsive to active Ras2, and adenylyl cyclase activity is no longer regulated by Ras2 in these cells (1, 2), indicating the involvement of CAP/srv2 in the Ras/cyclase pathway. However, some mutant CAP/srv2 alleles presented phenotypes not observed in strains with impaired Ras/cyclase pathway (1–3), indicating the existence of Ras/cyclase-independent functions downstream of CAP/srv2. These two phenotype groups, that is, Ras/cyclase-linked and Ras/cyclase-independent, could be suppressed by expression of an N-terminal half and a C-terminal half of CAP/srv2, respectively (4). Subsequent studies showed that the C-terminal half of CAP/srv2 was able to bind monomeric G-actin (5–8) and other actin regulators establishing a role in F-actin dynamics (9–16). Thus, CAP/srv2 is a bifunctional protein with an N-terminal domain involved in Ras/cyclase regulation and a C-terminal domain involved with F-actin dynamics regulation (16–18).

CAP1 is structurally conserved in all eukaryotes (18–22); however, their functions are not. Expression of the closely related *Schizosaccharomyces pombe* cap or mammalian CAP1 in yeast can only suppress the phenotypes associated with deletion of CAP/srv2's C-terminal but not its N-terminal domain (19, 20, 22), suggesting that only the F-actin dynamics function was conserved while the Ras/cyclase regulation diverged early on in evolution (16–18). CAP/srv2's N-terminal 1 to 36 domain was sufficient for cyclase binding in yeast involving a conserved RLE motif with predicted coiled-coil folding (23). Interestingly, this domain is also involved in CAP1 oligomerization both in yeast and mammalian cells (24–26), where it purifies as a high-molecular complex of ~600 kDa consistent with a 1:1 stoichiometric CAP1-actin hexameric organization (12, 25, 27, 28). Importantly, removal of this domain disrupted CAP1 oligomerization, reduced F-actin turnover in vitro and caused defects in cell growth, cell morphology, and F-actin organization in vivo (24, 29). However, whether the conserved RLE motif in mammalian CAP1 interacts with other coiled-coil–containing proteins is for the moment unknown.

Ras2-mediated cyclase regulation in yeast requires its farnesylation (30–32). However, the lipid target involved was not identified in the original studies. We have recently shown that mammalian CAP1 interacts with the small GTPase Rap1. The interaction involves Rap1's C-terminal hypervariable region (HVR) and its lipid moiety in a geranylgeranyl-specific manner; that is, neither the closely related Ras1 nor engineered farnesylated Rap1 interacted with CAP1 (33). Thus, we raised the question whether CAP1-Rap1, similar to CAP/srv2-Ras2 in yeast, plays a role in cAMP dynamics in mammalian cells.

In this study, we report that CAP1 binds to and activates mammalian adenylyl cyclase in vitro. The interaction involves

Significance

cAMP is a second messenger present in most cells, synthesized by adenylyl cyclase. Different isoforms are present in eukaryotes with distinct modes of regulation. In yeast, cyclase is regulated by Ras2 in a CAP1-dependent manner. CAP1 is conserved in mammals; however, its cyclase regulatory component is considered to be lost during evolution. We show that CAP1 binds and activates mammalian cyclase and reveal a role for Rap1, a CAP1 partner, in cyclase regulation in mammalian cells. These findings indicate that Rap1 is not just a downstream cAMP player but in the context of CAP1 is able to modulate cAMP synthesis, establishing a positive feedback that might provide mechanistic clues into the spatiotemporal regulation of G_s-dependent cAMP signaling.

Author contributions: X.Z., A.P., N.N., and D.L.A. designed research; X.Z., A.P., K.H., and D.L.A. performed research; C.Q. and V.K. contributed new reagents/analytic tools; X.Z., A.P., N.N., V.K., and D.L.A. analyzed data; and X.Z., A.P., and D.L.A. wrote the paper.

The authors declare no competing interest.

This article is a PNAS Direct Submission.

[1]X.Z. and A.P. contributed equally to this work.

[2]Present address: Large Molecule Drug Product Development Janssen Research & Development, L.L.C., Janssen Pharmaceutical Companies of Johnson & Johnson, Spring House, PA 19477.

[3]Present address: Scientific Support, Addgene, Watertown, MA 02472.

[4]To whom correspondence may be addressed. Email: altschul@pitt.edu.

This article contains supporting information online at https://www.pnas.org/lookup/suppl/doi:10.1073/pnas.2024576118/-/DCSupplemental.

Published June 7, 2021.

CAP1's conserved RLE motifs and cyclase's conserved catalytic subdomains (e.g., C1a and/or C2a). Most importantly, we show that both CAP1 and Rap1 modulate cAMP dynamics in live cells and are critical players in cAMP-dependent proliferation.

Results

CAP1 Interacts with Mammalian Adenylyl Cyclase Isoforms via Their Homologous C1 and C2 Catalytic Domains. CAP1 can be separated into two subdomains: a helical N-terminal (1 to 318) and a β-sheet C-terminal (319 to 475) subdomain. We expressed mammalian adenylyl cyclase isoforms in HEK cells and performed pull-down assays with *Escherichia coli* purified GST-fusion proteins of full-length, N- or C-CAP1 to determine interactions. Representative results are presented in Fig. 1*A*, showing interactions of all isoforms tested with N-CAP but not C-CAP. The decreased binding observed for full-length CAP1 is most likely attributed to known autoproteolysis (*SI Appendix*, Fig. S1) (33, 34). Since the two cyclase catalytic subdomains (e.g., C1a and C2a), homologous between them and conserved among all the cyclase isoforms, represent the only common domains (35, 36), we tested whether they could be responsible for the interaction with CAP1. Binding of an epitope-tagged C1–C2 fusion construct (37, 38) to immobilized GST-N-CAP or GST control proteins confirmed these domains are sufficient for interaction (Fig. 1*B*). To address if the interaction is direct, binding of N-CAP immobilized on beads was tested with purified His-C1a or His-C2 fragments derived from AC7. As shown in Fig. 1*C*, N-CAP associated directly with both C1a and C2 fragments either alone or in combination, suggesting that both subdomains, either independently or together are responsible for the CAP1-cyclase interaction. Microscale thermophoresis (MST) was then implemented to quantify the equilibrium dissociation constants of N-CAP and the C1a fragment. To accomplish this, purified N-CAP proteins were labeled in vitro with maleimide-NT647 and titrated with increasing amounts of the purified C1a fragment revealing a submicromolar affinity (K_D ~0.7 ± 0.1 μM). Similar results were observed with NH2 reagent NHS-NT647 (*SI Appendix*, Fig. S2). Taken together, these results provide evidence that CAP1 physically interacts with the highly conserved C1 and C2 catalytic loops and suggests the potential involvement of CAP's N-terminal domain for this interaction.

CAP1-Cyclase Interaction Involves CAP1's N-Terminal Coiled-Coil Domain. We then decided to map the binding domain within N-CAP responsible for its association with the cyclase catalytic domain/s. A deletion approach was implemented to test the binding properties of progressively smaller GST-fusion fragments of N-CAP immobilized on beads with purified His-C1a and His-C2 proteins. As can be seen in Fig. 2*A*, all fragments containing the N-terminal 2 to 41 region of N-CAP were able to bind to C1a and C2, while deletion of this domain in the context of N-CAP abolishes interaction. Similarly to N-CAP, CAP1 (2 to 41) binds both C1a (K_D ~1.1 ± 0.41μM) and C2 (K_D ~2.3 ± 0.50 μM) when evaluated by MST (Fig. 2*B*). To further map the residues within the aa2 to 41 region responsible for the interaction, a peptide array was designed, where 15-mer peptides covering this sequence (Δ3 amino acid shift) were spotted on membranes and binding to purified GST-IC1IIC2 was revealed with anti–GST-horseradish peroxidase (HRP) antibodies. As shown in Fig. 2*C*, only peptides covering the aa5 to 25 region (peptides #2, 3, and 4) of CAP1 (2 to 42) were able to interact with the C1–C2 fusion construct. Interestingly, peptides #2 and #3 contain the highly conserved "RLE motif" that forms a coiled-coil structure and is responsible for the interaction of CAP1 with cyclase in *Saccharomyces cerevisiae* (18, 31). In order to directly assess whether these RLE motifs are involved in binding, single residues in both motifs were changed to alanine in the context of the peptide #3 sequence, and the peptide array assay was repeated. Only the arginine and leucine residues in each one of the submotifs were required for this interaction, while the glutamate substitution did not affect the interaction (Fig. 2*D*). However, when tested in the context of the CAP1 (2 to 41) (Fig. 2*E*) or CAP1-FL (Fig. 2*F*), only the leucine residues in both RLE submotifs (L11S and L18S) were required for the interaction

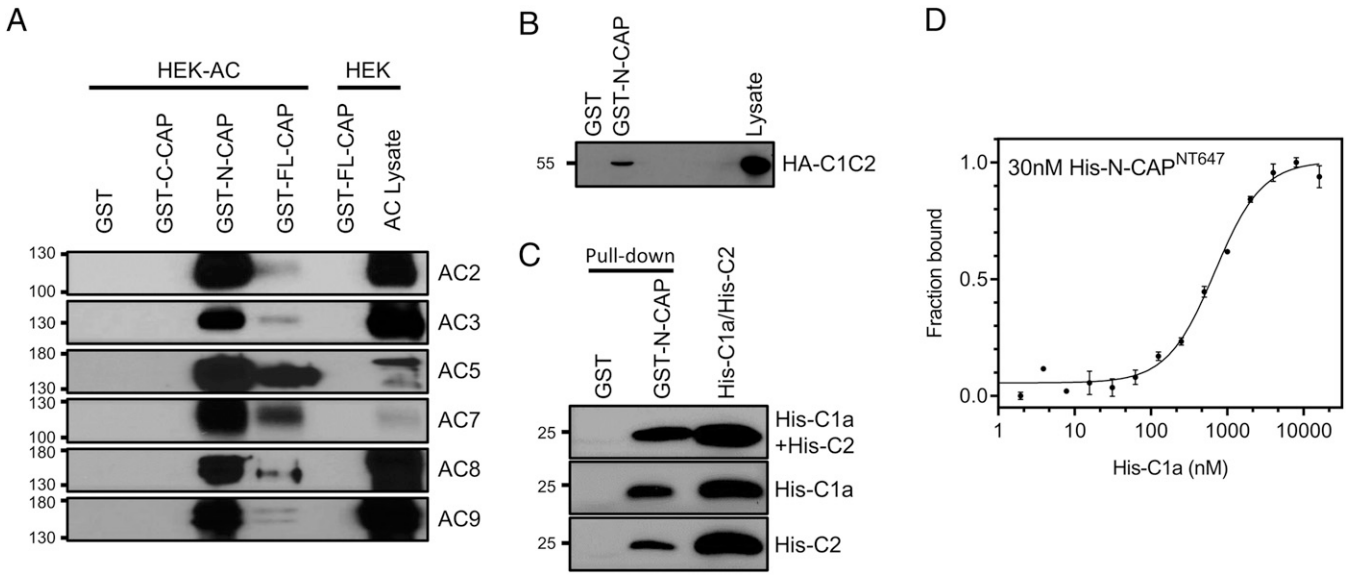

Fig. 1. CAP1-adenylyl cyclase interaction requires N-CAP (2-318) and cyclase conserved catalytic loops. (*A*) All cyclase isoforms tested interact with N-CAP. GST or GST-CAP1 proteins (25 μg) were immobilized onto Glutathione Sepharose 4B beads, and binding to lysates prepared from HEK cells transfected with epitope-tagged cyclase plasmids were assessed by Western blots using anti-Flag (AC5, AC7, AC8, AC9), anti-HA (AC2), or anti-AC3 antibodies. (*B*) CAP1 interacts with IC1a-IIC2a fusion protein. Immobilized GST or GST-N-CAP proteins were incubated with lysates from HEK cells transfected with soluble IC1a-IIC2a (HA-C1C2), and binding was assessed by Western blots with anti-HA antibody. (*C*) CAP1 interacts with either C1a or C2 domains. Immobilized GST or GST-N-CAP proteins were incubated with purified His-C1a (AC7; 1 μg) or His-C2 (AC7; 1 μg), and binding was assessed by Western blots with an anti-His antibody. All immunoblots are representative of three independent experiments. (*D*) MST analysis of in vitro NT647-Maleimide labeled His-N-CAP1 (30 nM) with purified His-C1a (AC7) as titrant. Data are expressed as mean ± SEM (n = 3).

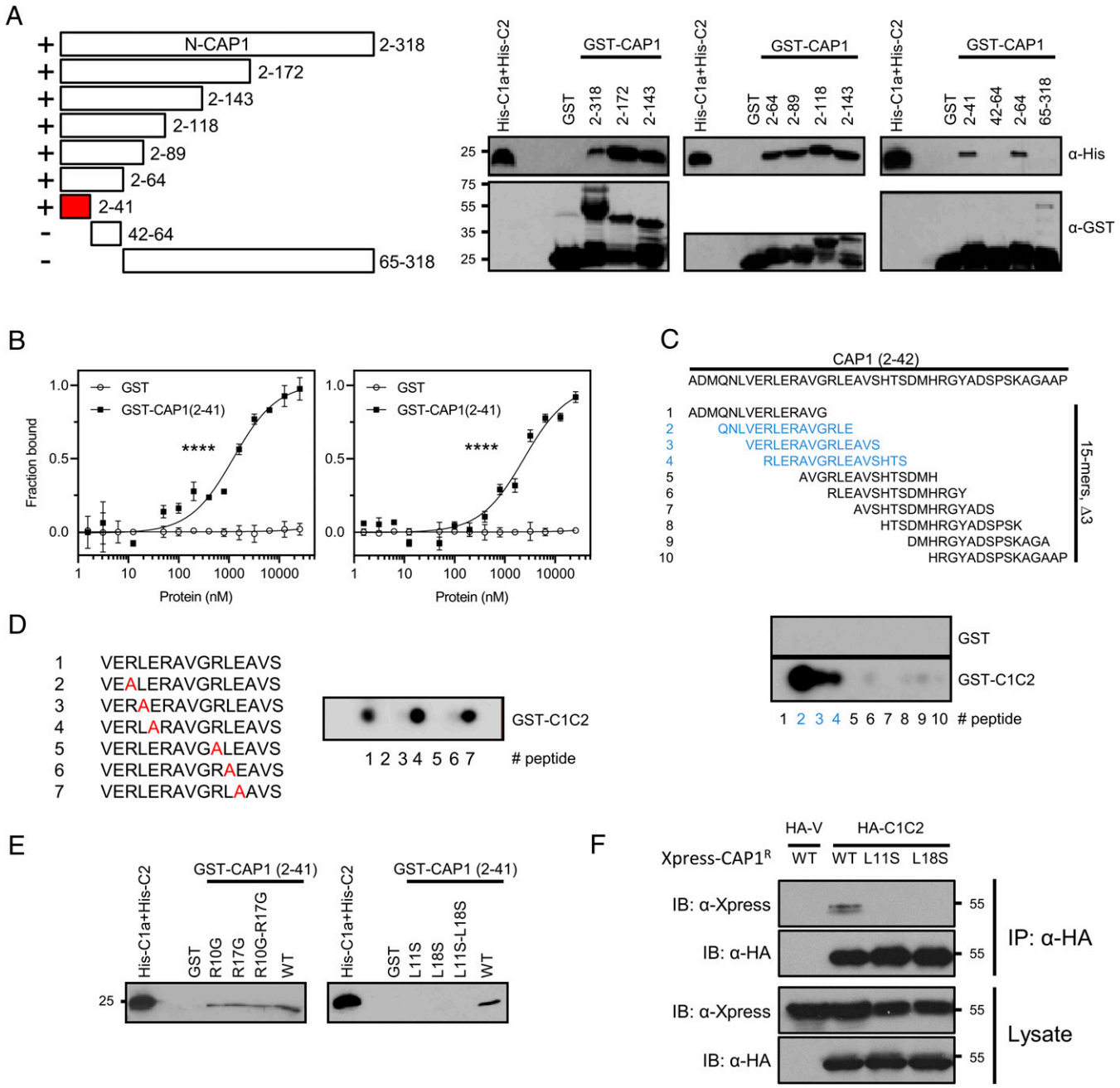

Fig. 2. CAP1-cyclase interaction involves CAP1's N-terminal coiled-coil domain. (*A*) CAP1 (2 to 41) contains the C1–C2 binding domain. Immobilized GST or GST-N-CAP deletion proteins were incubated with 1 μg purified His-C1a and His-C2, and binding was assessed by Western blots with an anti–His-tag antibody. (*B*) MST analysis of in vitro RED-Tris-NTA labeled His-C1a (*Left*, AC7; 100 nM) or His-C2 (*Right*, AC7; 100 nM) with purified GST-CAP1 (2 to 41) or GST alone as titrants. (*C*) Peptide array–based mapping. Peptides covering the CAP1 (2 to 41) sequence (15-mers, Δ3 amino acid shift) were spotted on membranes, incubated with purified GST-IC1IIC2, and binding was revealed by anti–GST-HRP antibody. (*D*) Alanine mutagenesis (peptide array format) identifies the involvement of the RLE motifs in binding to GST-IC1IIC2. (*E*) Leucine residues in CAP1 (2 to 41) RLE motifs are required for binding C1 and C2. Immobilized GST and GST-CAP (2 to 41) RLE mutants were incubated with purified His-C1a (AC7; 1 μg) and His-C2 (AC7; 1 μg), and binding was assessed by Western blots with an anti-His antibody. (*F*) Leucine residues in both RLE submotifs (L11S and L18S) are required for the interaction of full-length CAP1 with the soluble IC1a-IIC2a (HA-C1C2) fusion construct. Lysates from cells cotransfected with Xpress-tagged WT or mutant CAP1 and with HA-C1C2 were analyzed by HA-immunoprecipitation coupled to anti-Xpress blotting. All immunoblots and peptide arrays are representative of three independent experiments. MST data are expressed as mean ± SEM ($n = 3$). Significance tested was performed using a two-tailed Student's *t* test against GST control group (****$P < 0.001$).

with the C1–C2 fusion construct. Thus, these combined results indicate that a specific region within CAP1 N-terminal coiled-coil domain can interact with the C1–C2 catalytic loops of cyclase.

CAP1 Modulates Adenylyl Cyclase Activity In Vitro. Prompted by the binding results, we next assessed whether CAP1 binding was able to modulate cyclase activity. For these assays, we utilized the minimal C1–C2 fusion construct that is activated by forskolin addition in vitro (38). Forskolin activated GST-IC1IIC2 with an EC_{50} ~52 μM (Fig. 3*A*). Addition of purified GST-CAP1, but not GST control, modulated cyclase activity in a dose-dependent manner (Fig. 3*B*). Forskolin was strictly required to manifest the

effect of CAP1 on cyclase activity (*SI Appendix*, Fig. S3). Interestingly, compared to full-length CAP1, addition of GST-CAP1 (2 to 41), the minimal domain interacting with cyclase did not activate while GST-N-CAP1, only partially activated cyclase despite its binding ability (*SI Appendix*, Fig. S3). Forskolin dose responses were then performed to characterize the effect of CAP1 on cyclase activation. As shown in Fig. 3*C*, CAP1 affected the maximal response, without significant changes in EC50s. Next, we assessed whether CAP1 affected GαS-mediated activation of cyclase, its physiological activator. As shown in Fig. 3*D*, GST-CAP1, but not GST control, positively modulated GαS-GTPγS–mediated activation of C1C2, and similar to forskolin, it affected the maximal response without significant changes in EC50s. Thus, these results indicate that CAP1 can positively modulate forskolin and GαS-GTPγS–mediated cyclase activation in vitro and show that binding and activation can be functionally uncoupled.

CAP1 Expression Modulates cAMP Dynamics in Cells. Next, we assessed whether CAP1-cyclase interaction has functional consequences over cAMP dynamics in mammalian cells. We performed these experiments using PCCL3 thyroid follicular cells, a cAMP-responsive cell line we extensively studied (39–42). Real-time cAMP was monitored using the fluorescence resonance energy transfer (FRET)-based cAMP sensor, H188 (43), under conditions where CAP1 expression levels were positively (CAP1 overexpression) or negatively (sh-CAP1) modulated. The effects of CAP1 expression levels were evaluated by incremental ligand titration (*SI Appendix*, Fig. S4) and dose–response curves generated using a receptor-mediated agonist (TSH, thyroid stimulating hormone), a direct cyclase activator (FK, forskolin), and a nonselective PDE (phosphodiesterase) inhibitor (IBMX, 3-isobutyl-1-methylxanthine). In all cases examined, a marked left shift in dose responses was observed in CAP1 transfected cells when compared with vector-transfected cells (Fig. 4*A*). Correspondingly, sh-CAP1–mediated CAP1 down-regulation resulted in a right shift in the dose responses for the same ligands (Fig. 4*A*). Differences were most notably marked in forskolin-stimulated samples with EC_{50} ~0.008 ± 0.0004 μM and 0.15 ± 0.02 μM, and Hill coefficients ~2.1 ± 0.15 and 0.9 ± 0.1 for CAP1 and sh-CAP1, respectively. Moreover, CAP1 down-regulation diminished forskolin-stimulated cyclase activity in cells (Fig. 4*B*). Thus, these results demonstrate that CAP1 effectively modulates cAMP levels and provides evidence in favor of a CAP1-mediated modulation of cAMP dynamics in mammalian cells.

Rap1 Activation Modulates cAMP Dynamics in Mammalian Cells. Previous work from our laboratory provided evidence of a high-affinity interaction between CAP1 and the processed small GTPase Rap1 (33). To assess whether Rap1-GTP might be also involved in cAMP

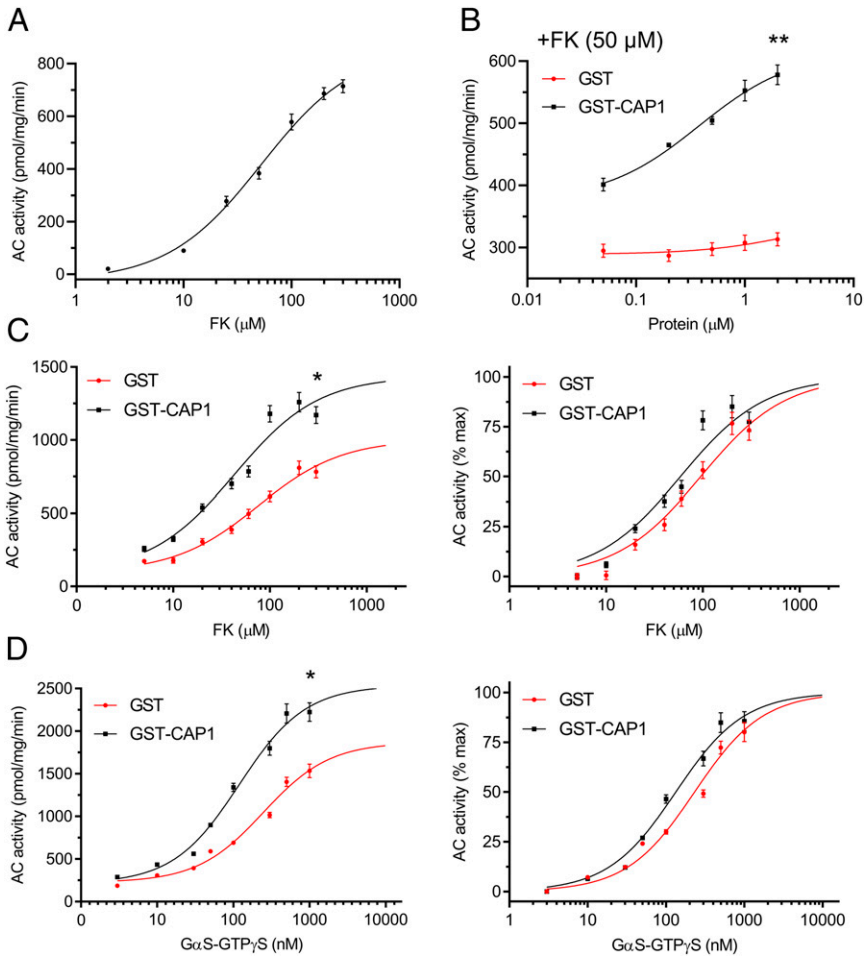

Fig. 3. CAP1 modulates adenylyl cyclase activity in vitro. AC activity was measured for 30 min/30 °C using purified GST-IC1IIC2 (50 nM) and ATP/Mg^{2+} as substrate. (*A*) Forskolin activates purified GST-IC1IIC2 (EC_{50} ~52 ± 3 μM). (*B*) CAP1 modulates cyclase activity in a dose-dependent manner measured as described with 50 μM forskolin. Effect of CAP1 on forskolin (*C*) and GαS dose responses (*D*). *Right* in *C* and *D* show normalized data (% max). Data (mean ± SEM) was normalized to GST control and analyzed by one-way ANOVA with Dunnett's multiple comparisons test against GST control group (*$P < 0.05$; **$P < 0.01$). All AC activity measurements are representative of at least three independent experiments.

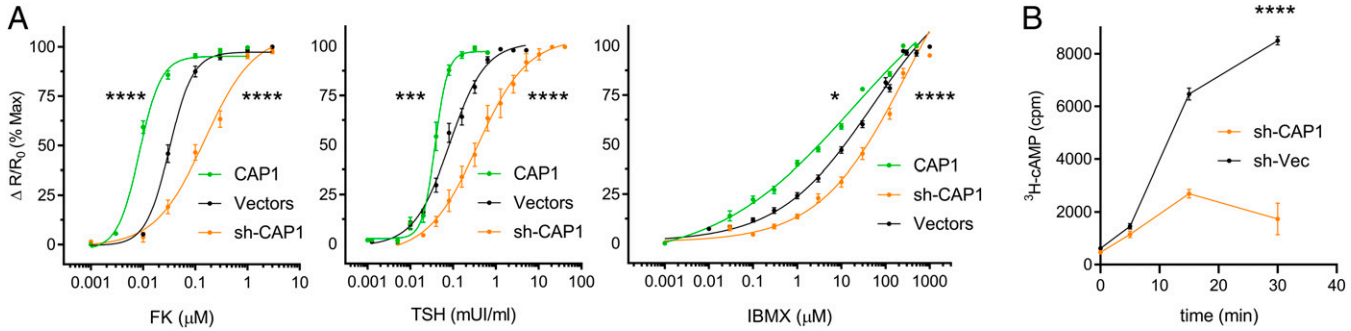

Fig. 4. CAP1 expression modulates cAMP dynamics in live cells. (*A*) The effect of CAP1 overexpression (CAP1) or down-regulation (sh-CAP1) in PCCL3 cells was assessed by stimulation with FK, TSH, and IBMX. Dose–response curves are expressed as the $\Delta R/R_0$ (% max) of the FRET response using the H188 sensor. Data are expressed as mean ± SEM, $n > 25$ cells from at least five independent coverslips. Curve fitting was performed in GraphPad Prism to extract EC_{50} and Hill coefficients and significance tested by a one-way ANOVA with Dunnett's multiple comparisons test against the vector control group (*$P < 0.05$; ***$P < 0.001$; ****$P < 0.0001$). (*B*) Cyclase activity and cAMP steady-state measurements in vector or sh-CAP1 transfected PCCL3 cells were evaluated after labeling the cellular pool of ATP with [^{3}H]-adenine and separation of [^{3}H]-cAMP product upon forskolin stimulation (1 μM) by sequential chromatography in Dowex/Alumina. Data are expressed as mean ± SD from at least three independent experiments.

dynamics, we performed dose responses as described above, in the presence of a negative Rap1 regulator, Rap-GAP (44, 45). As shown in Fig. 5*A*, Rap-GAP expression consistently inhibited the cAMP response generated by both FK and TSH, suggesting that Rap1-GTP is involved in the control of cAMP dynamics in cells, either stabilizing cAMP or affecting its rate of synthesis. An increase of cAMP levels upon addition of the broad PDE inhibitor IBMX reflects an increase in basal rate of synthesis. We reasoned, therefore, that a positive effect of a constitutively active Rap1 on cAMP levels upon IBMX stimulation could be used to dissect the effects of Rap1 on cAMP stabilization via PDE inhibition versus synthesis by adenylyl cyclase activation. IBMX dose responses performed on PCCL3 cells cotransfected with the H188 sensor and the constitutively active Rap1-G12V manifested a significant left shift in the curves (Fig. 5*A*), thus confirming a positive effect of Rap1-GTP on cAMP basal rate of synthesis. Moreover, consistent with the effects on cAMP dynamics, forskolin-stimulated cyclase activity in PCCL3 cells stably expressing Rap1-G12V was consistently higher than parental WT (wild type)-PCCL3 cells (Fig. 5*B*). Finally, we addressed the interdependency of CAP1-Rap1 actions on cAMP dynamics; Fig. 5*C* shows that the effects of Rap1-G12V can be negatively modulated by down-regulation of CAP1 (sh-CAP1) and reciprocally that the effect of CAP1 overexpression is negatively modulated by Rap1-GTP inactivation via Rap-GAP. Together, these results strongly suggest that Rap1 is acting not only as a downstream effector of cAMP (46, 47) but also in the CAP1-Rap1 context, as a potent upstream modulator of cAMP synthesis in PCCL3 cells.

CAP1 Modulates Downstream cAMP Effectors. Having established a role for CAP1 in cAMP levels, we next addressed whether cAMP effectors, Epac1 and PKA, were affected as well. A similar approach described above, that is, CAP1 overexpression and sh-CAP1–mediated down-regulation, were exploited to determine whether CAP1 expression levels could modify the consequences of cAMP signaling over two of its downstream effectors, PKA and Epac1. The overall effects on PKA activity were assessed using an anti–phosphorylated-Ser/Thr PKA substrate antibody and immunoblotting, while Epac1 activity in cells was measured using GST-RalGDS-RBD pull-down assays to monitor Rap1-GTP levels, as reported before (33). As expected, reduction of CAP1 expression levels by sh-CAP1 consistently decreased PKA (Fig. 6*A*) and Epac1 activity (Fig. 6*B*) upon forskolin stimulation. We have previously reported that Rap1 is phosphorylated by PKA at Ser179 (46), and therefore, pS179 Rap1 could be also used as a reporter of PKA activity in cells. Utilizing an in-house developed specific anti-pS179 Rap1 antibody, we confirmed the effects of sh-CAP1 (Fig. 6*C*) and CAP1 overexpression (Fig. 6*D*) on PKA activation upon forskolin stimulation. Thus, consistent with the effects on cAMP levels, these results underline the functional relevance of CAP1 on the activation of downstream cAMP effectors.

CAP1 Is Required for TSH-Mediated Cell Proliferation. PCCL3 thyroid cells represent a well-established model to study cAMP-dependent proliferation, and we have previously reported that the trophic hormone TSH works via a synergistic response utilizing both cAMP effectors, that is, Epac1-mediated Rap1 activation and PKA-mediated Rap1 phosphorylation (39, 40). We reasoned, therefore, that the described effects of CAP1-Rap1 on cAMP dynamics should be reflected as a requirement for TSH on S-phase entry.

Exploiting that both sh-Vector and sh-CAP1 plasmids express an independent dsRed unit, we performed a BrdU incorporation assay monitoring % BrdU/dsRed at a single-cell level (*SI Appendix*, Fig. S4), as reported before (39, 41). As shown in Fig. 7, an effective down-regulation of CAP1 expression was confirmed by immunoblotting (Fig. 7*A*), and CAP1 down-regulation consistently blocked TSH-mediated G_1/S progression. Moreover, this effect was CAP1 specific as evidenced by rescue assays performed with sh-resistant CAP1 expressing plasmids (Fig. 7*B*). As expected from our previous studies (33), constitutively active pS179-Rap1-G12V was not able to rescue the inhibitory action of sh-CAP1 (*SI Appendix*, Fig. S5). Next, we repeated the rescue assay in the presence of a sh-resistant CAP1 mutant bearing the L11S or L18S substitutions shown above to block CAP1-cyclase interaction. Consistent with the effects on binding, these mutations were unable to rescue TSH-mediated G_1/S progression (Fig. 7*C*). Thus, these results show that CAP1 and its RLE-containing coiled-coil domain involved in cyclase interaction is required for TSH/cAMP-mediated cell proliferation.

Discussion

CAP1, originally identified in yeast (1, 2), is conserved in all eukaryotes (17, 18). Two functions were originally described that both genetically and biochemically associated with distinct CAP1 domains. While N-CAP1 binds to and regulates the Ras-cyclase pathway, its C-CAP1 domain was associated with regulation of F-actin dynamics. Even though CAP1-mediated regulation of the actin cytoskeleton is present and was extensively studied in mammalian cells, it is accepted in the field that during evolution the Ras-cyclase branch was lost and therefore is no longer

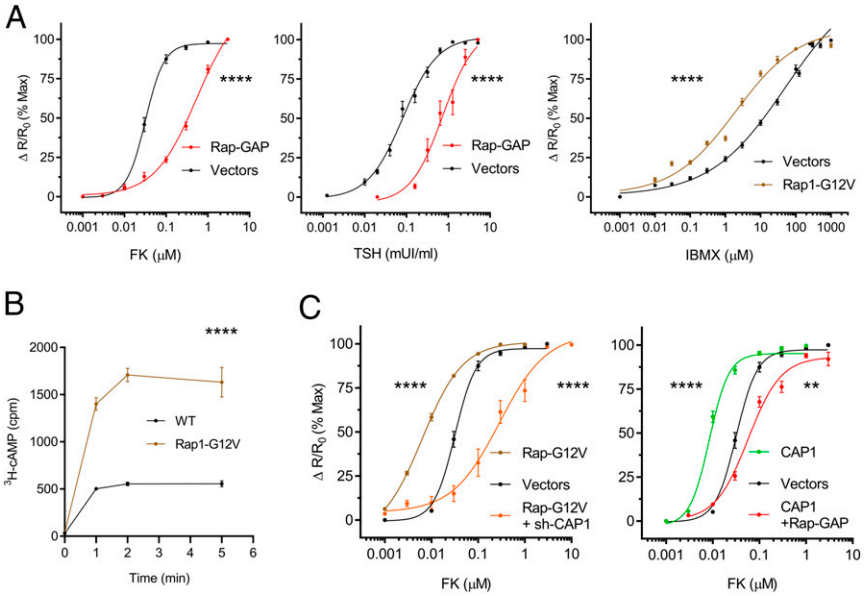

Fig. 5. Rap1 modulates cAMP dynamics in live cells. (*A*) The effect of active Rap1-GTP in cAMP dynamics was assessed by expression of the negative regulator Rap-GAP in PCCL3 cells upon stimulation with FK or TSH (*Left*). The effect of constitutively active Rap1-G12V on cAMP dynamics was assessed upon stimulation with IBMX (*Right*). (*B*) Cyclase activity and cAMP steady-state determination in PCCL3 cells (WT), and cells stably transfected with Rap1-G12V were measured as described in Fig. 4. Data are expressed as mean ± SD from at least three independent experiments. (*C*) The combined effect of constitutively active Rap1-G12V and CAP1 down-regulation (sh-CAP1) on cAMP dynamics was assessed upon stimulation with FK (*Left*). Also, the combined effect of Rap-GAP and CAP1 overexpression (CAP1) was tested (*Right*). Dose–response curves of *A* and *C* are expressed as the ΔR/R0 (% max) of the FRET response using the H188 sensor (mean ± SEM, $n > 14$ cells from at least four independent coverslips). Curve fitting was performed in GraphPad Prism to extract EC_{50} and Hill coefficients, and significance was tested using a two-tailed Student's *t* test against vector control group (**$P < 0.01$; ****$P < 0.001$).

observed in higher eukaryotes (16, 17). In this report, we provide evidence that CAP1 binds to and activates mammalian cyclase in vitro and modulates cAMP dynamics in mammalian cells, albeit in a Rap1-dependent manner.

We describe here that CAP1 interacts with all cyclase isoforms tested suggesting the common catalytic loops as targets; indeed, both purified C1 and C2 interact with a submicromolar affinity to an N-terminal fragment of CAP1. Using a combination of deletion, peptide array, and mutagenesis approaches we have identified a pair of leucine residues at CAP's N-terminal domain (L11 and L18) as critical elements in cyclase binding. These residues are present in highly conserved RLE (Arg-Leu-Glu) repeats, predicted to form a coiled-coil folding unit due to the presence of canonical heptad units (48). This predicts the existence of a conserved helix in C1/C2, exposed and with propensity to form helical coiled coils. A single helix satisfying all these properties (human AC5-C1, ^{489}ELVMTLNELF) scored positive in public coiled-coil prediction algorithms (49). Interestingly, this domain in cyclase/s is involved in Gαi (α2 helix/C1) and GαS (α2' helix/C2) interactions (50). Although both homologous C1 and C2 domains are able to interact with CAP1 in vitro, the ability of CAP1 to increase GαS-mediated IC1-IIC2 activation in a noncompetitive way (i.e., at high GαS concentration) strongly argues for CAP1 interacting with helix α2 on the C1a interface. Current mutagenesis/binding assays are ongoing to confirm α2-C1a′s involvement and identify potential contact residues, that is, a single residue interfering with CAP1-cyclase interaction without disrupting its basal forskolin activation profile.

CAP1 from yeast and mammals purifies as a large complex of ~600 kDa, consistent with an oligomeric organization formed by six CAP and six G-actin monomers (16). Purified N-CAP1 forms tetramers and hexamers in vitro (24, 29, 51), and this higher-order structure requires the presence of an oligomerization domain that overlaps with the coiled-coil cyclase binding domain identified here. A possibility is that in cells, CAP1 exists in equilibrium between hexameric and monomer/dimers, the latter able to interact with cyclase. Moreover, since the oligomerization domain-dependent hexameric evidence comes from purified N-CAP1 alone, and C-CAP1 is known to dimerize as well as interact with N-CAP1 (7, 52–55), alternative in vivo configurations satisfying the ~600 kDa oligomeric structure while leaving a free N-terminal coiled-coil available for cyclase binding cannot be disregarded. Therefore, whether CAP1's oligomerization state is necessary for cyclase regulation, as clearly established for CAP1 modulation of F-actin dynamics (16, 17), is still unknown.

We also show that CAP1 can directly enhance the activity of a C1–C2 fusion enzyme (i.e., the minimal catalytic unit necessary for cAMP synthesis) but only when activated by either forskolin or its physiological regulator GαS indicating that CAP1 action is not simply stabilizing C1–C2 loops. Also, CAP1 does not significantly affect forskolin-AC or GαS–AC affinity interaction, and although the mechanism of CAP1-mediated activation is for the moment unknown, the proximity of α2-C1a to the catalytic pocket (ATP binding site) of cyclase might suggest a direct effect on the active site of the enzyme. Moreover, binding is not sufficient for full activation, since fragments that bind to C1–C2 did not activate (e.g., CAP1 2–41), or only partially activated (e.g., N-CAP1), the C1–C2 enzyme. This suggests a second low affinity site located beyond N-CAP1 might be required for activation or, alternatively, that full-length CAP1 supports the formation of an oligomeric structure that adopts a conformation essential for full activation. Regardless of the mechanism involved, and despite the recent report of a CAP1-cyclase complex in pancreatic cells (56), this study demonstrates that solely the presence of CAP1 can modify cyclase activity in vitro. However, several limitations of our initial approach need to be acknowledged. First, a suboptimal activation could be associated with the use of the minimal C1–C2 catalytic construct as opposed to a full-length cyclase. Second, although CAP1's coiled-coil domain supports binding to all cyclases tested, we do not know whether isoform-specific

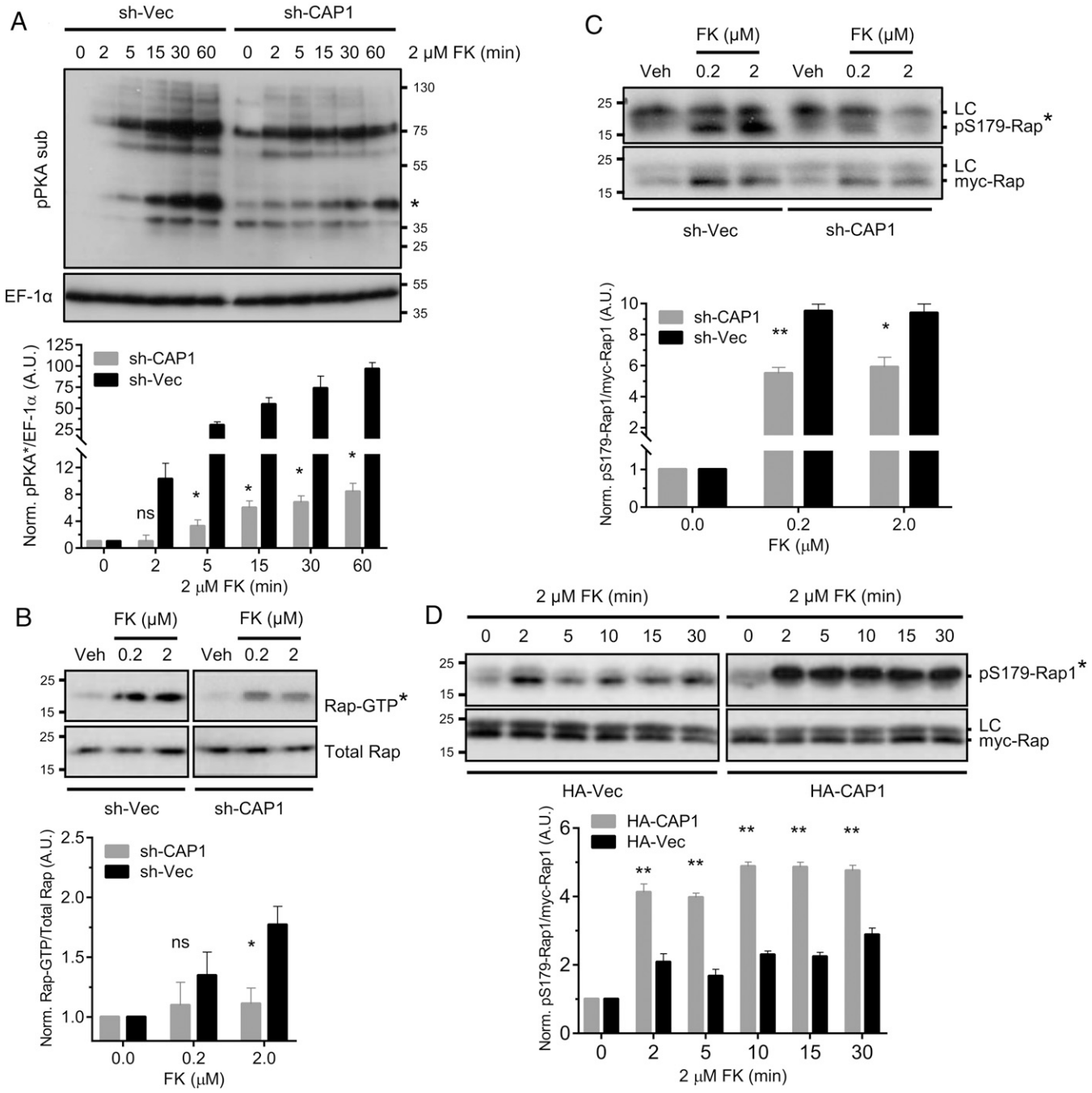

Fig. 6. CAP1 modulates cAMP effectors Epac1 and PKA. (*A*) Effect of CAP1 down-regulation (sh-CAP1) on FK-stimulated PKA activity assessed by blots with anti-PKA substrate antibody. (*B*) Effect of CAP1 down-regulation (sh-CAP1) on FK-stimulated Epac1-mediated Rap1 activation assessed by RalGDS-RBD pull-down assays. (*C*) Effect of CAP1 down-regulation (sh-CAP1) on FK-stimulated myc-Rap1 phosphorylation using an anti-pS179 Rap1 antibody (LC, light chain). (*D*) Effect of CAP1 expression (HA-CAP1) on FK-stimulated myc-Rap1 phosphorylation using an anti-pS179 Rap1 antibody (LC, light chain). The density of each band was measured using the integrated density volume divided by EF-1α, total Rap1, or myc-Rap, respectively, to account for differences in loaded amounts and protein expression. Then, all measurements were normalized to their respective control experiment. Data (mean ± SEM) were obtained from at least three independent experiments and significance tested using a two-tailed Student's *t* test against the respective control group (*$P < 0.05$; **$P < 0.01$). A.U., arbitrary units.

activation might be present. Third, other regulatory factors missing in our in vitro reconstitution assay (e.g., Rap1) might be necessary for full activation. Ongoing experiments are addressing these limitations.

Most importantly, using FRET-based cAMP sensors, we can recapitulate CAP1 action on cAMP dynamics in live cells. Utilizing ligands able to increase cAMP by different mechanisms all involving cyclase activation (i.e., TSH, Forskolin, and IBMX), we can show that modulation of CAP1 expression levels correlates with expected shifts in their dose–response curves. Several points are worth noting. CAP1 down-regulation does not block ligand-mediated cAMP accumulation but rather affects potency, indicating CAP1 is not strictly required for cyclase activation but represents a component in its regulation. Moreover, differences in Hill coefficients are revealed

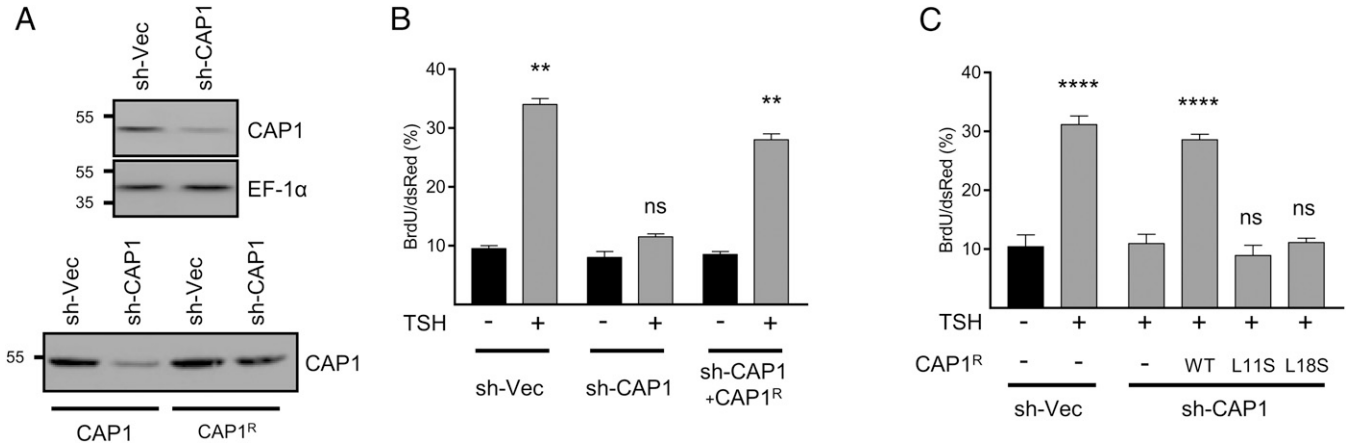

Fig. 7. CAP1 down-regulation blocks cAMP-mediated G_1/S progression. (*A*) Efficient down-regulation of CAP1 by shRNA. PCCL3 cells were transfected with CAP1 shRNA (sh-CAP1) or empty vector (sh-Vec). Endogenous CAP1 expression was tested by Western blot using a CAP1-specific antibody. EF-1α signal was used as loading control (*Top*). Expression of HA-tagged shRNA-resistant ($CAP1^R$) or shRNA-sensitive CAP1 (CAP1) in PCCL3 cells cotransfected with sh-Vec or sh-CAP1. After 72 h, cells were lysed, and CAP1 was detected using an HA-specific antibody (*Lower*). (*B*) PCCL3 cells were transfected with pSiren-red-sh-CAP1 (sh-CAP1) or empty vector (sh-Vec), and BrdU labeling was used to monitor TSH-dependent G_1/S progression in the presence of 10% FBS as comitogen. The inhibitory response can be rescued with a sh-resistant CAP1 ($CAP1^R$). (*C*) RLE $CAP1^R$ mutants L11S and L18S unable to bind cyclase cannot rescue proliferation. Data are expressed as % BrdU/dsRed (mean ± SEM, $n \geq 110{,}000$ cells from at least three independent coverslips) and significance tested using a two-tailed Student's *t* test (ns, nonsignificant; $^{**}P < 0.01$; $^{****}P < 0.0001$).

consistent with a potential role of CAP1 in organizing a cyclase dimeric/oligomeric structure.

We have previously shown, both in cell lines in vitro as well as in vivo in transgenic mice, that the small GTPase Rap1 is involved in cAMP-dependent proliferation, involving a synergistic collaboration of cAMP effectors, Epac1 and PKA (39, 40, 42, 44, 57). Recently, we showed that Rap1, but not Ras, interacts with CAP1; the interaction involves C-CAP1's β-barrel domain and Rap1's C-terminal HVR in a geranylgeranyl-specific manner (33). Interestingly, like the effects of CAP1 on cAMP dynamics, we show that interventions that modulate Rap1 activity correlate with changes in cAMP production as assessed by dose–response curves and activity assays in live cells. The effects of CAP1 and Rap-GTP overexpression seem to be interdependent since sh-CAP1 blocks the effect of Rap-GTP, and Rap-GAP blocks the action of CAP1 overexpression. Similarly, like Rap1's involvement in cAMP-dependent proliferation, we show here that CAP1 is also involved in TSH-mediated proliferation of PCCL3 cells in a coiled-coil domain-dependent manner. Thus, we propose the cyclase-CAP1-Rap1 unit represents a key regulatory component in the cAMP-dependent proliferative response.

Our findings indicate that Rap1 is not just a downstream cAMP player, but in the context of CAP1, is able to modulate cAMP's rate of synthesis. We advance the hypothesis that the cyclase-CAP1-Rap1 complex establishes a positive feedback loop acting as a signal amplifier, manifested both as an increased dynamic range (maximum response) as well as an increased sensitivity to inducer signals (potentiation). Identification of the cyclase isoform target and physical compartment action might aid in understanding the mechanistic basis for the establishment of cAMP microdomains and localized signaling (58, 59).

Besides the well-established role of CAP1 in actin cytoskeleton dynamics, the recent findings of new CAP1 partners indicate its potential participation in unforeseen biological responses. CAP1 was recently identified as a potential receptor and mediator of resistin-induced cAMP increase and NFkB-mediated transcriptional regulation of proinflammatory cytokines (60). Moreover, CAP1 binding to PCSK9 was recently involved with internalization and lysosome trafficking of LDL receptors (61). Interestingly, recent reports also involved Rap1 in lysosomal biology (62, 63), raising the question of whether CAP1-Rap1 might also be involved in these responses.

Materials and Methods

Materials. TSH, forskolin, IBMX, C12E9, Dowex and alumina resins, and anti-FLAG antibody were from Sigma. GSH-agarose was from GE Healthcare Life Sciences. [2,8-^{3}H] Adenine was from PerkinElmer. Ni-NTA agarose was from QIAGEN. Antibodies against HA (HA.11) and myc (9E10) were from Covance. Anti-AC3 antibody was from EnCor Biotechnology Inc. Anti-GST antibody (A5800) and anti-Xpress antibody were from Invitrogen. Anti–phospho-(Ser/Thr) PKA substrate antibody was from Cell Signaling. Anti-CAP1 antibody was from Proteintech, and anti-His antibody was from Aviva Systems Biology.

Cell Lines and Transfections. PCCL3, a normal TSH-dependent rat thyroid follicular cell line, was grown in 5% Coon's modified F-12 medium (Sigma) supplemented with 5% fetal bovine serum (FBS) and the combination of four hormones: TSH (1 mIU/mL; IU, international units), insulin (1 μg/mL), transferrin (5 μg/mL), and hydrocortisone (1 nM), as described before (39, 40). HEK-293T cells were maintained in Dulbecco's modified Eagle's medium (Cambrex) supplemented with 10% FBS. Cells were kept at 37 °C in 5% CO_2, 95% humidified air environment. Transfections were performed using Lipofectamine 3000 Transfection kit (Invitrogen) for PCCL3 cells or X-tremeGENE HP DNA Transfection Reagent (Roche) for HEK-293T cells adjusting the total amount of DNA plasmid to 0.5 to 1 μg/well as directed by the manufacturers.

DNA Constructs. pCGN-HA-Rap1, HA-Rap1-G12V, HA-CAP1, and sh-CAP1 constructs were already described (33). small hairpin RNA (shRNA)-resistant CAP1 was a gift from Dr. Guolei Zhou, Arkansas State University, Jonesboro, AR (64). GST-CAP1 full-length, GST-N-CAP1 (2 to 318), and GST-C-CAP1 (319 to 475) were prepared by inserting SalI-XhoI PCR fragments into pGEX-5X-2 using HA-CAP1 as a template. GST-CAP1 (2 to 41) (2 to 64) (2 to 89) (2 to 118) (2 to 143) (2 to 172) (65 to 318) constructs were made through inserting EcoRI-XhoI PCR fragments into pGEX-5X-2 using GST-N-CAP1 as a template. GST-IC1IIC2 was prepared by subcloning a BamHI/XhoI fragment from pCMV-HA-IC1a-IIC2a (37) into pGEX-4T-1. GST-CAP1 (2 to 41) -R10G, -R17G, -R10G-R17G, -L11S, -L18S, and -L11S-L18S, as well as sh-resistant $CAP1^R$-L11S and $CAP1^R$-L18S were constructed by site-directed mutagenesis. Epitope-tagged (HA-AC2 and FLAG-AC5, AC-7, AC-8 and AC-9) and untagged (AC3) adenylyl cyclases were provided by Drs. Jiang and Dessauer. PCR products from Flag-AC7 were digested with NdeI-HdIII and subcloned into pET-28c, generating His-C1a and His-C2, using the following primers:

C1a-Forward: 5′-agctagctcatatgcctgacaacaacttccac-3′

C1a- Reverse: 5′-agctagctaagcttttacagggccgcgtccccttggg-3′

C2-Forward: 5′-agctagctcatatggacaagttaaacgaggactgg-3′

C2-Reverse: 5′-agctagctaagcttttagttcagccccagcccctgaaa-3′.

Protein Purification. Rosetta (DE3) competent *E. coli* cells transformed with the appropriate pGEX or pET28c plasmids were grown until OD_{600} >1.0 and induced for 16 h at 24 °C with 0.5 mM IPTG. Cells were harvested and lysed in lysis buffer: 50 mM Tris, pH 7.5, 150 mM NaCl, 10% glycerol, 1% Triton-X100, 0.2 mg/mL lysozyme, and 1× PMSF. After centrifugation, supernatants were subjected to affinity chromatography on GSH-Sepharose (GE Healthcare) or Ni-NTA agarose (QIAGEN), respectively. Similarly, GαS-8xHis expressed in High Five insect cells was solubilized in 1% dodecyl-b-maltoside and purified on Ni-NTA agarose, as described before (65). Nucleotide loading is performed by addition of 0.1mM GTPγS, 10mM $MgCl_2$ at 30 °C for 1 h.

GST Pull-Downs. A total of 1 mL bacteria lysates containing GST or GST-fusion proteins were mixed by rotation with 40 μl 50% GSH-Sepharose at 4 °C for 1 h. The Glutathione Sepharose beads were briefly centrifuged and washed three times with lysis buffer: 25 mM Tris, pH 7.5, 150 mM NaCl, 5 mM MgCl2, 5% glycerol, 1% Nonidet P-40. Lysates from HEK transfected with cyclase isoforms were prepared in 0.2% C12E19 and 5 μl (5 to 10 μg/μl) added to the beads in 800 μl binding buffer (50 mM Tris, pH 7.5, 150 mM NaCl, 0.003% C12E9) for 1 h at 4 °C with shaking. After washing the beads three times with the same binding buffer, associated proteins were eluted, resolved on SDS-PAGE (sodium dodecyl sulphate–polyacrylamide gel electrophoresis), and analyzed by Western blots with specific antibodies. For binding to His-C1a + His-C2, 1 to 2 μg of purified His-fusion proteins were used under the conditions described above.

Immunoprecipitation. sh-resistant $CAP1^R$-L11S and $CAP1^R$-L18S were cotransfected with HA-IC1a-IIC2a in HEK-293T cells. After 48 h, cells were lysed with a buffer containing 50 mM Tris/Cl pH 7.5, 50 mM NaCl, 0.5% Nonidet P-40, 5% glycerol, and protease inhibitors. Lysates were incubated for 1 h at 4 °C with HA-agarose beads (Thermo Fisher Scientific) followed by four washes with lysis buffer and blotting with Xpress antibody.

Rap1 Activation Assay Using RalGDS-RBD. Cells transfected with a plasmid expressing HA-Rap1b were lysed with a buffer containing 25 mM Tris/Cl pH 7.5, 150 mM NaCl, 1% Nonidet P-40, 5% glycerol, 5 mM $MgCl_2$, and protease inhibitors. Lysates were clarified by centrifugation at 13,000 rpm for 10 min at 4 °C. Purified GST-RalGDS-RBD precoupled to Glutathione Sepharose beads (10 μg) was added to the supernatants and incubated at 4 °C for 60 min with agitation. Beads were washed four times in the same lysis buffer. After the final wash, Laemmli sample buffer was added to the samples. Proteins were fractionated in a 12% SDS-PAGE and transferred to a polyvinylidene difluoride membrane for blotting.

Peptide Arrays. Peptides encompassing CAP1 2 to 42 (15-mers, Δ3) for the original peptide scan and peptides with specific substitution replacements were synthesized and spotted on trioxatridecanediamine cellulose membranes (three polyethylene glycol units as linker between cellulose and peptides) using services provided by Kinexus Bioinformatics Corporation. Binding to purified GST-IC1IIC2 was revealed with anti-GST-HRP antibodies following their protocols (66).

MST. Labeling of His-N-CAP1 proteins with NT647-Maleimide and NT647-NHS, or His-C1a and His-C2 with RED-Tris-NTA second generation fluorescent dyes followed the protocols provided by NanoTemper. Briefly, 20 μM purified proteins were mixed with 60 μM dye in a volume of 100 μl. The labeling mixture was incubated for 30 min at room temperature in the dark. Free dye was removed through the column from the kit. The thermophoresis measurements were performed in a Monolith NT.115 instrument with blue/red channels (Nanotemper) using Premium coated capillaries (Nanotemper, Catalog MO-K005). For experiments with His-C1a binding to His-N-CAP1, samples were prepared in MST binding buffer (1× phosphate-buffered saline (PBS), 0.05% Tween-20, 0.05% Pluronic F-127, 0.05 mg/mL bovine serum albumin [BSA]). His-N-CAP1 was used at a final concentration of 30 nM, and measurements were performed at 14% light-emitting diode (LED) and 60% MST power. Dose responses in triplicates (mean ± SEM) were analyzed with the unit software or upon import into GraphPad Prism.

cAMP Determination Assay. cAMP determination follows the manufacturers' protocol (Cyclic AMP XP Assay Kit, Cell Signaling) with slight modifications. Briefly, a 10 μL mix was prepared containing 0.4 μg purified GST-IC1IIC2, forskolin, and recombinant GST-CAP1 or GST control, and pre-equilibrated for 10 min at room temperature. Then, 90 μl assay buffer (50 mM Hepes pH 7.2, 5 mM MgCl2, 1 mM ATP) was added, and after 30 min at 30 °C, the reaction was terminated by the addition of 1.5 μL concentrated HCL, followed by 50 μl 0.4 M Tris (pH 8.8) for neutralization. Aliquots of this mix were tested following exactly the protocol provided in the kit.

Adenylyl Cyclase Activity in Cells. Labeling of cellular ATP pool was performed by overnight incubation with 1 mCi/mL [3H] adenine in complete Coon's medium. The next day, cells were washed twice and incubated for 1 h in Coon's starvation medium. Cells were then stimulated with forskolin (1 μM) and IBMX (100 μM) for the indicated time and reactions stopped in trichloroacetic acid (7.5% weight/volume). Product [^{3}H]cAMP was separated from substrate [^{3}H]ATP by sequential column chromatography over Dowex and alumina, as described (67).

FRET-Based Dose–Response cAMP Measurements. PCCL3 cells were seeded on 25-mm glass coverslips and transfected with the FRET sensor H188 (43). Transfected cells were given fresh media for 72 h and hormone starved for 3 h in starvation Coon's media (lacking TSH, insulin, and hydrocortisone) containing 5% FBS before measurements. Cells were washed once in PBS and imaged in OptiMEM media lacking phenol red (Gibco) on an Olympus IX70 microscope equipped with a Till Polychrome V monochromator. Images were acquired every 10 s with a 60×/1.4 NA oil objective, 8 × 8 binning, and a Hamamatsu charge-coupled device (CCD) camera (Photonics Model C4742-80-12AG) using Slidebook software 6 (Intelligent Imaging Innovations Inc.). The H188 sensor was excited at 440 nm (20% intensity) and fluorescence collected using emission filters 470/30 nm and 535/30 nm with dichroic 86002v1 (Chroma Technology Corp.). Fluorescence was corrected for channel bleed through (~53%) and direct acceptor excitation (~3%). No significant photobleaching was observed during the time lapses using monochromator at 20% max. Dose responses were performed by treating cells with increasing concentrations of TSH, FSK, and IBMX. A final incubation with saturating doses of FK and IBMX (20 and 250 μM, respectively) was performed in every experiment to rule out sensor saturation. Initially, changes in background-subtracted FRET ratios (R) relative to resting conditions (R/R0) were calculated. Traces were then normalized using the resting R/R0 values (without agonist; 0%) and the maximal R/R0 values (saturating dose of either TSH, FSK, or IBMX; 100%) (*SI Appendix*, Fig. S4). Finally, traces were fitted with the four-parameter logistic equation in GraphPad Prism 8 (GraphPad Software Inc.). EC_{50} and Hill coefficients were estimated and significance tested using a two-tailed Student's *t* test or by one-way ANOVA with Dunnett's multiple comparisons tests when appropriate (α level was defined as 0.05).

BrdU Labeling. Cells were grown to 70% confluency on glass coverslips, transfected with sh-Vector or sh-CAP1 plasmids for 56 h, and made quiescent by serum starvation in Coon's/5% FBS for 16 h. Upon agonist stimulation (5% FBS/TSH) for 8 h, cells were labeled for 16 h with BrdU (Sigma, 100 μM). At the end of the labeling period, cells were fixed in 4% paraformaldehyde (10 min, room temperature) and permeabilized with 0.5% Triton X-100 (10 min, room temperature). After washing, incorporated BrdU was detected by indirect immunofluorescence. Samples were stained for 30 min at 37 °C with sheep anti-BrdU antibody (Biodesign International; diluted 1/100 in PBS/3% BSA) in the presence of RQ1 DNase (Promega; 10 units/mL). After washing, samples were incubated for 30 min at 37 °C with a combination of 488-conjugated goat-anti-sheep (Invitrogen, dilution, 1/150 in PBS/3% BSA) and DAPI (0.125 mg/mL, Invitrogen). After extensive washes, samples were mounted in PermaFluor (Thermo) and imaged using the same setup described in the previous section. Both sh-Vector and sh-CAP1 were cloned in a pSIREN vector containing an independent-driven cassette for expression of dsRed Express. Data are expressed as %BrdU (green)/dsRed Express (red) and significance tested using a two-tailed Student's *t* test (α level was defined as 0.05).

Data Availability. All study data are included in the article and/or *SI Appendix*.

ACKNOWLEDGMENTS. We thank Drs. Lily Jiang and Carmen Dessauer for the adenylyl cyclase expression plasmids, Dr. Troy Stevens for the soluble HA-IC1a-IIC2a construct, and Dr. Guolei Zhou for the sh-resistant mtCAP1 plasmid. Funding was provided by NIH Grants R01 GM099775 and GM130612 to D.L.A.

1. J. Field *et al.*, Cloning and characterization of CAP, the *S. cerevisiae* gene encoding the 70 kd adenylyl cyclase-associated protein. *Cell* **61**, 319–327 (1990).
2. M. Fedor-Chaiken, R. J. Deschenes, J. R. Broach, SRV2, a gene required for Ras activation of adenylate cyclase in yeast. *Cell* **61**, 329–340 (1990).
3. A. Vojtek *et al.*, Evidence for a functional link between profilin and CAP in the yeast *S. cerevisiae*. *Cell* **66**, 497–505 (1991).
4. J. E. Gerst, K. Ferguson, A. Vojtek, M. Wigler, J. Field, CAP is a bifunctional component of the *Saccharomyces cerevisiae* adenylyl cyclase complex. *Mol. Cell. Biol.* **11**, 1248–1257 (1991).

5. S. Iwase, S. Ono, Conserved hydrophobic residues in the CARP/β-sheet domain of cyclase-associated protein are involved in actin monomer regulation. *Cytoskeleton (Hoboken)* **74**, 343–355 (2017).
6. T. Lila, D. G. Drubin, Evidence for physical and functional interactions among two *Saccharomyces cerevisiae* SH3 domain proteins, an adenylyl cyclase-associated protein and the actin cytoskeleton. *Mol. Biol. Cell* **8**, 367–385 (1997).
7. A. Zelicof *et al*., Two separate functions are encoded by the carboxyl-terminal domains of the yeast cyclase-associated protein and its mammalian homologs. Dimerization and actin binding. *J. Biol. Chem.* **271**, 18243–18252 (1996).
8. G. L. Zhou, H. Zhang, H. Wu, P. Ghai, J. Field, Phosphorylation of the cytoskeletal protein CAP1 controls its association with cofilin and actin. *J. Cell Sci.* **127**, 5052–5065 (2014).
9. A. B. Johnston, A. Collins, B. L. Goode, High-speed depolymerization at actin filament ends jointly catalysed by Twinfilin and Srv2/CAP. *Nat. Cell Biol.* **17**, 1504–1511 (2015).
10. T. Kotila *et al*., Mechanism of synergistic actin filament pointed end depolymerization by cyclase-associated protein and cofilin. *Nat. Commun.* **10**, 5320 (2019).
11. M. Makkonen, E. Bertling, N. A. Chebotareva, J. Baum, P. Lappalainen, Mammalian and malaria parasite cyclase-associated proteins catalyze nucleotide exchange on G-actin through a conserved mechanism. *J. Biol. Chem.* **288**, 984–994 (2013).
12. K. Moriyama, I. Yahara, Human CAP1 is a key factor in the recycling of cofilin and actin for rapid actin turnover. *J. Cell Sci.* **115**, 1591–1601 (2002).
13. M. A *et al*., Regulation of INF2-mediated actin polymerization through site-specific lysine acetylation of actin itself. *Proc. Natl. Acad. Sci. U.S.A.* **117**, 439–447 (2020).
14. K. P. M. Normoyle, W. M. Brieher, Cyclase-associated protein (CAP) acts directly on F-actin to accelerate cofilin-mediated actin severing across the range of physiological pH. *J. Biol. Chem.* **287**, 35722–35732 (2012).
15. S. Shekhar, J. Chung, J. Kondev, J. Gelles, B. L. Goode, Synergy between cyclase-associated protein and cofilin accelerates actin filament depolymerization by two orders of magnitude. *Nat. Commun.* **10**, 5319 (2019).
16. M. B. Rust, S. Khudayberdiev, S. Pelucchi, E. Marcello, CAPt'n of actin dynamics: Recent advances in the molecular, developmental and physiological functions of cyclase-associated protein (CAP). *Front. Cell Dev. Biol.* **8**, 586631 (2020).
17. S. Ono, The role of cyclase-associated protein in regulating actin filament dynamics - more than a monomer-sequestration factor. *J. Cell Sci.* **126**, 3249–3258 (2013).
18. A. V. Hubberstey, E. P. Mottillo, Cyclase-associated proteins: CAPacity for linking signal transduction and actin polymerization. *FASEB J.* **16**, 487–499 (2002).
19. M. Kawamukai *et al*., Genetic and biochemical analysis of the adenylyl cyclase-associated protein, cap, in *Schizosaccharomyces pombe*. *Mol. Biol. Cell* **3**, 167–180 (1992).
20. H. Matviw, G. Yu, D. Young, Identification of a human cDNA encoding a protein that is structurally and functionally related to the yeast adenylyl cyclase-associated CAP proteins. *Mol. Cell. Biol.* **12**, 5033–5040 (1992).
21. A. B. Vojtek, J. A. Cooper, Identification and characterization of a cDNA encoding mouse CAP: A homolog of the yeast adenylyl cyclase associated protein. *J. Cell Sci.* **105**, 777–785 (1993).
22. A. Zelicof, J. Gatica, J. E. Gerst, Molecular cloning and characterization of a rat homolog of CAP, the adenylyl cyclase-associated protein from *Saccharomyces cerevisiae*. *J. Biol. Chem.* **268**, 13448–13453 (1993).
23. Y. Nishida *et al*., Coiled-coil interaction of N-terminal 36 residues of cyclase-associated protein with adenylyl cyclase is sufficient for its function in *Saccharomyces cerevisiae* Ras pathway. *J. Biol. Chem.* **273**, 28019–28024 (1998).
24. V. Purde, F. Busch, E. Kudryashova, V. H. Wysocki, D. S. Kudryashov, Oligomerization affects the ability of human cyclase-associated proteins 1 and 2 to promote actin severing by cofilins. *Int. J. Mol. Sci.* **20**, E5647 (2019).
25. O. Quintero-Monzon *et al*., Reconstitution and dissection of the 600-kDa Srv2/CAP complex: Roles for oligomerization and cofilin-actin binding in driving actin turnover. *J. Biol. Chem.* **284**, 10923–10934 (2009).
26. J. Yu, C. Wang, S. J. Palmieri, B. K. Haarer, J. Field, A cytoskeletal localizing domain in the cyclase-associated protein, CAP/Srv2p, regulates access to a distant SH3-binding site. *J. Biol. Chem.* **274**, 19985–19991 (1999).
27. H. I. Balcer *et al*., Coordinated regulation of actin filament turnover by a high-molecular-weight Srv2/CAP complex, cofilin, profilin, and Aip1. *Curr. Biol.* **13**, 2159–2169 (2003).
28. M. A, T. S. Fung, A. N. Kettenbach, R. Chakrabarti, H. N. Higgs, A complex containing lysine-acetylated actin inhibits the formin INF2. *Nat. Cell Biol.* **21**, 592–602 (2019).
29. S. Jansen, A. Collins, L. Golden, O. Sokolova, B. L. Goode, Structure and mechanism of mouse cyclase-associated protein (CAP1) in regulating actin dynamics. *J. Biol. Chem.* **289**, 30732–30742 (2014).
30. Y. Kuroda, N. Suzuki, T. Kataoka, The effect of posttranslational modifications on the interaction of Ras2 with adenylyl cyclase. *Science* **259**, 683–686 (1993).
31. F. Shima *et al*., Association of yeast adenylyl cyclase with cyclase-associated protein CAP forms a second Ras-binding site which mediates its Ras-dependent activation. *Mol. Cell. Biol.* **20**, 26–33 (2000).
32. F. Shima *et al*., Effect of association with adenylyl cyclase-associated protein on the interaction of yeast adenylyl cyclase with Ras protein. *Mol. Cell. Biol.* **17**, 1057–1064 (1997).
33. X. Zhang *et al*., Cyclase-associated protein 1 (CAP1) is a prenyl-binding partner of Rap1 GTPase. *J. Biol. Chem.* **293**, 7659–7673 (2018).
34. A. Hofmann, S. Hess, A. A. Noegel, M. Schleicher, A. Wlodawer, Crystallization of cyclase-associated protein from Dictyostelium discoideum. *Acta Crystallogr. D Biol. Crystallogr.* **58**, 1858–1861 (2002).
35. J. Bassler, J. E. Schultz, A. N. Lupas, Adenylate cyclases: Receivers, transducers, and generators of signals. *Cell. Signal.* **46**, 135–144 (2018).
36. C. W. Dessauer *et al*., International union of basic and clinical pharmacology. CI. Structures and small molecule modulators of mammalian adenylyl cyclases. *Pharmacol. Rev.* **69**, 93–139 (2017).
37. S. L. Sayner, M. Alexeyev, C. W. Dessauer, T. Stevens, Soluble adenylyl cyclase reveals the significance of cAMP compartmentation on pulmonary microvascular endothelial cell barrier. *Circ. Res.* **98**, 675–681 (2006).
38. W. J. Tang, A. G. Gilman, Construction of a soluble adenylyl cyclase activated by Gs alpha and forskolin. *Science* **268**, 1769–1772 (1995).
39. D. Hochbaum, G. Barila, F. Ribeiro-Neto, D. L. Altschuler, Radixin assembles cAMP effectors Epac and PKA into a functional cAMP compartment: Role in cAMP-dependent cell proliferation. *J. Biol. Chem.* **286**, 859–866 (2011).
40. D. Hochbaum, K. Hong, G. Barila, F. Ribeiro-Neto, D. L. Altschuler, Epac, in synergy with cAMP-dependent protein kinase (PKA), is required for cAMP-mediated mitogenesis. *J. Biol. Chem.* **283**, 4464–4468 (2008).
41. N. Naim *et al*., Luminescence-activated nucleotide cyclase regulates spatial and temporal cAMP synthesis. *J. Biol. Chem.* **294**, 1095–1103 (2019).
42. F. Ribeiro-Neto, J. Urbani, N. Lemee, L. Lou, D. L. Altschuler, On the mitogenic properties of Rap1b: cAMP-induced G(1)/S entry requires activated and phosphorylated Rap1b. *Proc. Natl. Acad. Sci. U.S.A.* **99**, 5418–5423 (2002).
43. J. Klarenbeek, J. Goedhart, A. van Batenburg, D. Groenewald, K. Jalink, Fourth-generation epac-based FRET sensors for cAMP feature exceptional brightness, photostability and dynamic range: Characterization of dedicated sensors for FLIM, for ratiometry and with high affinity. *PLoS One* **10**, e0122513 (2015).
44. D. L. Altschuler, F. Ribeiro-Neto, Mitogenic and oncogenic properties of the small G protein Rap1b. *Proc. Natl. Acad. Sci. U.S.A.* **95**, 7475–7479 (1998).
45. B. Rubinfeld *et al*., Molecular cloning of a GTPase activating protein specific for the Krev-1 protein p21rap1. *Cell* **65**, 1033–1042 (1991).
46. D. Altschuler, E. G. Lapetina, Mutational analysis of the cAMP-dependent protein kinase-mediated phosphorylation site of Rap1b. *J. Biol. Chem.* **268**, 7527–7531 (1993).
47. D. L. Altschuler, S. N. Peterson, M. C. Ostrowski, E. G. Lapetina, Cyclic AMP-dependent activation of Rap1b. *J. Biol. Chem.* **270**, 10373–10376 (1995).
48. W. M. Park, Coiled-coils: The molecular zippers that self-assemble protein nanostructures. *Int. J. Mol. Sci.* **21**, E3584 (2020).
49. J. Ludwiczak, A. Winski, K. Szczepaniak, V. Alva, S. Dunin-Horkawicz, DeepCoil-a fast and accurate prediction of coiled-coil domains in protein sequences. *Bioinformatics* **35**, 2790–2795 (2019).
50. C. W. Dessauer, J. J. Tesmer, S. R. Sprang, A. G. Gilman, Identification of a Gialpha binding site on type V adenylyl cyclase. *J. Biol. Chem.* **273**, 25831–25839 (1998).
51. F. Chaudhry *et al*., Srv2/cyclase-associated protein forms hexameric shurikens that directly catalyze actin filament severing by cofilin. *Mol. Biol. Cell* **24**, 31–41 (2013).
52. T. Dodatko *et al*., Crystal structure of the actin binding domain of the cyclase-associated protein. *Biochemistry* **43**, 10628–10641 (2004).
53. A. Hubberstey, G. Yu, R. Loewith, C. Lakusta, D. Young, Mammalian CAP interacts with CAP, CAP2, and actin. *J. Cell. Biochem.* **61**, 459–466 (1996).
54. S. Iwase, S. Ono, The C-terminal dimerization motif of cyclase-associated protein is essential for actin monomer regulation. *Biochem. J.* **473**, 4427–4441 (2016).
55. T. Kotila *et al*., Structural basis of actin monomer re-charging by cyclase-associated protein. *Nat. Commun.* **9**, 1892 (2018).
56. S. N. Quinn *et al*., Adenylyl cyclase 3/adenylyl cyclase-associated protein 1 (CAP1) complex mediates the anti-migratory effect of forskolin in pancreatic cancer cells. *Mol. Carcinog.* **56**, 1344–1360 (2017).
57. F. Ribeiro-Neto *et al*., cAMP-dependent oncogenic action of Rap1b in the thyroid gland. *J. Biol. Chem.* **279**, 46868–46875 (2004).
58. N. Musheshe, M. Schmidt, M. Zaccolo, cAMP: From long-range second messenger to nanodomain signalling. *Trends Pharmacol. Sci.* **39**, 209–222 (2018).
59. T. C. Rich *et al*., Cyclic nucleotide-gated channels colocalize with adenylyl cyclase in regions of restricted cAMP diffusion. *J. Gen. Physiol.* **116**, 147–161 (2000).
60. S. Lee *et al*., Adenylyl cyclase-associated protein 1 is a receptor for human resistin and mediates inflammatory actions of human monocytes. *Cell Metab.* **19**, 484–497 (2014).
61. H. D. Jang *et al*., Cyclase-associated protein 1 is a binding partner of proprotein convertase subtilisin/kexin type-9 and is required for the degradation of low-density lipoprotein receptors by proprotein convertase subtilisin/kexin type-9. *Eur. Heart J.* **41**, 239–252 (2020).
62. A. P. Mutvei *et al*., Rap1-GTPases control mTORC1 activity by coordinating lysosome organization with amino acid availability. *Nat. Commun.* **11**, 1416 (2020).
63. L. Zhang *et al*., Ras and Rap signal bidirectional synaptic plasticity via distinct subcellular microdomains. *Neuron* **98**, 783–800.e4 (2018).
64. H. Zhang *et al*., Mammalian adenylyl cyclase-associated protein 1 (CAP1) regulates cofilin function, the actin cytoskeleton, and cell adhesion. *J. Biol. Chem.* **288**, 20966–20977 (2013).
65. C. Qi, S. Sorrentino, O. Medalia, V. M. Korkhov, The structure of a membrane adenylyl cyclase bound to an activated stimulatory G protein. *Science* **364**, 389–394 (2019).
66. D. F. Winkler, H. Andresen, K. Hilpert, SPOT synthesis as a tool to study protein-protein interactions. *Methods Mol. Biol.* **723**, 105–127 (2011).
67. Y. Salomon, C. Londos, M. Rodbell, A highly sensitive adenylate cyclase assay. *Anal. Biochem.* **58**, 541–548 (1974).